

# Self-Assembling Nano- and Microparticles of Chitosan L- and D-Aspartate: Preparation, Structure, and Biological Activity †

Anna Shipovskaya <sup>1,\*</sup> , Xenia Shipenok <sup>1</sup> , Tatiana Lugovitskaya <sup>2</sup>  and Tatiana Babicheva <sup>1</sup> 

<sup>1</sup> Institute of Chemistry, Saratov State University, 410012 Saratov, Russia; kshipenok@gmail.com (X.S.); tatyana.babicheva.1993@mail.ru (T.B.)

<sup>2</sup> Institute of New Materials and Technologies, Ural Federal State University, 620002 Ekaterinburg, Russia; tlugovitskaja@mail.ru

\* Correspondence: shipovskayaab@yandex.ru

† Presented at the 4th International Online Conference on Nanomaterials, 5–19 May 2023; Available online: <https://iocn2023.sciforum.net>.

**Abstract:** The paper considers the formative processes of chiral nano- and microparticles in solutions of D-aminoglucan chitosan (CS) in L- and D-aspartic acid (AspA) by means of the counterionic condensation of components and the stabilization of particles by a polysiloxane shell. The effect of the L- and D-enantiomers of AspA on the structure, size, shape, and zeta potential of nano(micro)particles was studied using IR spectroscopy, dynamic light scattering, and electron and optical microscopy. It was found that chiral particles of CS·L-AspA and CS·D-AspA are non-toxic, hemo- and biocompatible, and exhibit high growth-stimulating activity in the test plants, with the best effect observed for homochiral D-glucan–D-AspA particles.

**Keywords:** chitosan; aspartic acid; L- and D-enantiomers; nano(micro)particles; chirality; biological activity; growth-stimulating ability

## 1. Introduction

CS nano- and microparticles have very promising applications in biomedicine and biotechnology due to their non-toxicity, biodegradability, wide range of biologically valuable properties, and inexpensive raw materials [1–4]. The main properties and potential applications of nano(micro)particles of the D-aminoglucan analyzed herein significantly depend on its size, zeta potential, and morphological and surface characteristics, including with respect to the functionalization of the surface with a protective shell [1,2,4]. The small sizes of such nano(micro)particles and, accordingly, their large surface area provide significantly higher antimicrobial and antibacterial activity against various pathogenic bacteria and plant pathogens compared to the original polymer [4,5].

Some publications have noted great the prospects of using CS salts with biologically active carboxylic acids and amino acids to produce nano(micro)particles with improved properties. For example, CS ascorbate nanoparticles produced via ionotropic gelation with pentasodium tripolyphosphate were characterized by antioxidant, mucoadhesive, wound-healing, and antimicrobial properties, which were significantly better than those of a CS solution in ascorbic acid prepared at the same concentration of both the polymer and the acid [6,7]. Nanoparticles based on CS glutamate, aspartate, glycolate, and lactate that were also obtained through ionotropic gelation, but with sodium tripolyphosphate, showed high efficiency when loaded with bovine serum albumin [8]. In this case, the conformation of macrochains and the viscosity of the polymer in the aqueous acid solution used as the source significantly depended on the nature of the organic acid used, which, in turn, affected the dimensional, charge, and functional characteristics of the nanoparticles.

We have studied the biological activity of nano(micro)particles of CS L-aspartate formed in a CS + L-AspA + water system at the initial stage of phase separation through



**Citation:** Shipovskaya, A.; Shipenok, X.; Lugovitskaya, T.; Babicheva, T. Self-Assembling Nano- and Microparticles of Chitosan L- and D-Aspartate: Preparation, Structure, and Biological Activity. *Mater. Proc.* **2023**, *14*, 31. <https://doi.org/10.3390/IOCN2023-14492>

Academic Editor: Ullrich Scherf

Published: 5 May 2023



**Copyright:** © 2023 by the authors. Licensee MDPI, Basel, Switzerland. This article is an open access article distributed under the terms and conditions of the Creative Commons Attribution (CC BY) license (<https://creativecommons.org/licenses/by/4.0/>).

the mechanism of counterionic condensation [9]. It was established that the cultivation of *Staphylococcus aureus* 209 P and *Escherichia coli* 113-13 in a nutrient medium with the addition of these particles led to the massive death of the bacterial cultures, for which the highest biocidal effect was against Gram-positive bacteria. At the same time, in vitro biotesting conducted on the model of cell lines of human dermal fibroblasts and normal keratinocytes, as well as epitheliocytes of the embryonic kidney of the rhesus macaque MA-104, revealed the high biocompatibility of the particles and their ability to accelerate the proliferative activity of these epidermal and epithelial cell cultures. However, dispersions of such nano(micro)particles of CS L-aspartate were kinetically unstable because they form spontaneously due to phase segregation of the polymer substance [10]. In this regard, the task was set to stabilize these nano(micro)particles by forming a protective shell on their surface out of pharmacologically active silicon tetraglycerolate. In addition, since the nature of the solvent acid used, including the isomeric forms of the substance [8,11,12], significantly affects the biological activity of chitosan-containing materials obtained from solutions, not only L-AspA but also its D-enantiomer were used to form particles.

The purpose of this work was to obtain chiral nano(micro)particles of CS L- and D-asparaginate, functionalize their surfaces with a protective shell, and evaluate their size characteristics and some biological properties.

## 2. Experimental Section

### 2.1. Materials

The following reagents were used: CS with a viscosity average molecular weight of 200 kDa and a degree of deacetylation (DD) = 82 mol% (Bioprogress Ltd., St. Peterburg, Russia); L-AspA (JSC Bioamid, Moscow, Russia); D-AspA (Vekton Ltd., St. Peterburg, Russia); distilled water; and laboratory-synthesized silicon tetraglycerolate ( $\text{Si}(\text{OGly})_4$ ) obtained via the method described in Ref. [13]. All reagents were chemical grade and used without further purification.

### 2.2. Obtaining Nanoparticles

An Atlas reactor (Syrris, Royston, UK) was used. Distilled water (50 mL) was poured into a round-bottom flask and heated to 50 °C under stirring on a magnetic stirrer at 400 rpm; then, 0.3 g of CS was added, and the suspension was stirred for 20 min to allow the CS particles to swell. Then, 0.4 g of L- or D-AspA and 50 mL of distilled water were added. Stirring was continued under the same conditions for 3 h until the solids were completely dissolved, at which point they were filtered through a Schott-160 funnel. A total of 25 mL of the filtered CS solution was isolated in a separate round-bottom flask, ~0.08 g of  $\text{Si}(\text{OGly})_4$  was added, and the mixture was stirred at 50 °C for 6 h, as described above. The initial and modified (with a polysiloxane shell) colloidal solutions of CS in L- or D-AspA were stored for no more than  $t = 2$  days and no more than  $t = 300$  days, respectively.

### 2.3. Methods of Examination

Gravimetric measurements were carried out on an Ohaus Discovery analytical balance (USA) with a weighing accuracy of  $\pm 0.01$  mg.

pH was measured using a Mettler Toledo Five Easy FE20 pH meter (Germany).

The main characteristics (average diameter ( $d$ , nm), proportion of the predominant fraction of particles ( $Q$ , %), polydispersity index ( $P_i$ ), and electrokinetic potential ( $\zeta$ , mV)) of nanoparticles and the conductivity of their aqueous dispersions ( $\chi$ , mS/cm) were determined via dynamic light scattering (DLS) using complex equipment (Zetasizer Ultra Red Label Malvern Panalytical (Great Britain)) at  $23 \pm 2$  °C.

IR spectra were recorded on a Bruker Alpha IR Fourier spectrometer equipped with an ATR (ZnSe) attachment operating in the 500–4000  $\text{cm}^{-1}$  wavenumber range. Sample preparation was carried out as follows. The dispersion of nano(micro)particles was placed into a Petri dish, dried in an air atmosphere at  $23 \pm 2$  °C until an air-dried film was formed (i.e., 48 h), and crushed into powder with a particle size of ~150  $\mu\text{m}$ .

SEM images were taken on a MIRA\\LMU scanning electron microscope (Tescan, Brno, Czechia) equipped with an energy-dispersive detector (EDX) operating at a voltage of 30 kV and a conducting current of 400 pA. A 5 nm thick gold layer was deposited on each sample using a K450X Carbon Coater (DE). FIB-SEM images were obtained using a Thermo Scientific SCIOS 2 electron-ion (two-beam) scanning microscope operating at an accelerating voltage of 2 kV. A layer of gold was deposited onto each sample using a Jeol JEE-420 vacuum evaporator. During sample preparation for SEM and TEM, a drop of the nano(micro)particle dispersion was applied to a glass substrate and dried in an air atmosphere for 24 h.

#### 2.4. Study of Biological Properties

Hemocompatibility was assessed *in vitro* using a model of human erythrocytes under conditions conducive to the detection of oxidized hemoglobin forms according to the method described in Ref. [14]. Biocompatibility was studied *in vitro* using cell lines of human dermal fibroblasts and normal keratinocytes as well as epithelial cells of the embryonic kidney of the rhesus macaque MA-104 as models [10]. Antimicrobial and antifungal effects were studied *in vitro* using a daily culture model of the rhizospheric bacteria *Pseudomonas aureofaciens* cultivated in meat peptone broth (MPB) according to the procedure outlined in Ref. [9]. Bio-stimulating activity was tested *in vivo* using radish (*Raphanus sativus*) and white mustard (*Sinapis alba*) as test plants. Seventy-five seeds of these test plants were planted in open ground according to traditional methods of agricultural technology and grown for 25 days. Irrigation with the dispersion of nano(micro)particles and water (control) was carried out on the day of planting and then once every 2 days at the following rate: volume of irrigation liquid/volume of bed soil = 0.2. The growth-stimulating effect was assessed by examining seed germination and the height and weight of the vegetative shoots of the test plants.

For all experiments assessing biological activity, at least three parallel experiments were performed. Statistical data processing was carried out using Statistica 6.0.

### 3. Results and Discussion

#### 3.1. Preparation and Characterization of Nano(micro)particles of Chitosan L- and D-Aspartate

It has been established that chiral (enantio-enriched) salt complexes of CS with L- and D-AspA in aqueous solution exhibit the properties of a partially charge-compensated polyelectrolyte [10,11]. This hydrodynamic behavior indicates the implementation of a mixed polyelectrolyte–ionomer mode, wherein some of the HAsp<sup>−</sup> counterions are in an associated (bound) state with  $-\text{NH}_3^+$  groups of the macrochain entailing the formation of ion pairs (Figure 1a). It is thermodynamically unfavorable for counterions to be in a free state, and they continue to form ion pairs with  $-\text{NH}_3^+$  groups of polymer chains (ionomers), wherein they lose entropy but gain electrostatic energy (Figure 1b).

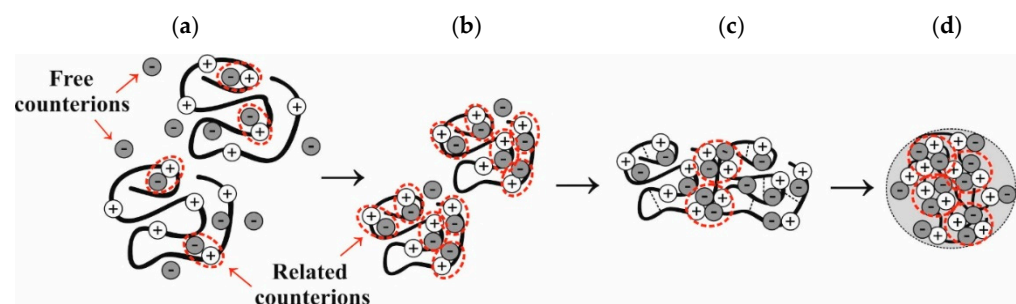


**Figure 1.** Distribution of free and bound counterions in the CS + AspA + H<sub>2</sub>O system during storage: (a) polycation with a partially compensated charge, (b) ion pairs, (c) multiplets, and (d) phase segregation of the polymer phase in the form of a nanoparticle.

The resulting effective attraction between monomer units contributes to the dipole–dipole interaction of ion pairs and their combination into multiplet structures (Figure 1c). It is most likely the case that the stabilization of the latter occurs through complex ion–ion–hydrogen interactions involving ionogenic groups of the CS aspartate macromolecule and the AspA molecule [10]. Multiplets function as physical crosslinks between different polymer chains, thereby contributing to the compaction of macrocoils and the formation of nanosized nuclei of a new phase (Figure 1d). Upon aggregation of the latter to micro and macroparticles, the metastable polymer system is divided into two equilibrium phases: the polymer-rich phase precipitates and the polymer-depleted phase, for which the latter is represented by the supernatant liquid.

To characterize the chiral nano(micro)particles formed in the CS + AspA + water system, we used two complementary methods: DLS and FIB-SEM.

According to DLS, the average size and zeta potential of the particles formed in a freshly prepared aqueous solution of CS in L-AspA were  $\sim 1.20 \mu\text{m}$  and  $\sim 38 \text{ mV}$ , respectively; those for CS in D-AspA were somewhat smaller, namely,  $\sim 0.75 \mu\text{m}$  and  $\sim 36 \text{ mV}$  (Table 1). (It should be noted that the effective radius of the macromolecular coil of these salt forms of CS was also larger for CS L-aspartate [11]). EDX analysis showed that the elemental composition of the polymer phase of the particles in an air-dried state consisted of  $42.95 \pm 1.2\%$  carbon,  $21.09 \pm 0.9\%$  nitrogen, and  $35.96 \pm 1.0\%$  oxygen. This, as well as the results presented in Ref. [10], proves that the microparticles are represented by the chiral salt form of the polymer, i.e., CS aspartate. The colloidal stability of the CS L- and D-aspartate microparticles formed at the initial stage of phase separation of the system under study did not exceed a period of 24–48 h.

**Table 1.** Physicochemical characteristics of the CS + L-(D-)AspA + water system and size characteristics of chiral particles of chitosan L- and D-aspartate obtained via DLS.

System			<i>t</i> , days	$\chi$ , mS/cm	Particle Characteristics			
CS Salt	Modifier	pH			<i>d</i> , nm	<i>Q</i> , %	<i>P<sub>i</sub></i>	$\zeta$ , mV
CS + L-AspA	–	4.5	–	0.74	$1200 \pm 300$	$80 \pm 8$	$0.60 \pm 0.25$	$38 \pm 3$
			–	0.73	$1500 \pm 100$	$94 \pm 2$	$0.40 \pm 0.05$	$37 \pm 2$
			14	0.71	$1500 \pm 100$	$92 \pm 2$	$0.40 \pm 0.05$	$37 \pm 2$
	Si(OGly) <sub>4</sub>	3.6	40	0.70	$1500 \pm 100$	$90 \pm 3$	$0.40 \pm 0.05$	$37 \pm 2$
			300	0.73	$1200 \pm 200$	$95 \pm 4$	$0.40 \pm 0.20$	$36 \pm 1$
CS + D-AspA	–	4.5	–	0.70	$750 \pm 150$	$94 \pm 3$	$0.90 \pm 0.10$	$36 \pm 1$
			–	0.70	$1000 \pm 100$	$92 \pm 2$	$0.90 \pm 0.20$	$33 \pm 3$
	Si(OGly) <sub>4</sub>	3.5	55	0.73	$1200 \pm 200$	$76 \pm 2$	$0.50 \pm 0.10$	$35 \pm 1$
			125	0.68	$1500 \pm 400$	$66 \pm 2$	$0.60 \pm 0.10$	$31 \pm 1$

To eliminate the low aggregative stability of the CS L- and D-aspartate particles, their surfaces were dynamically modified and simultaneously functionalized according to the corresponding core–shell type due to electrostatic forces. Pharmacologically active silicon tetraglycerolate was used as a sol–gel precursor for the first time [13]. An analysis of Table 1 shows that the average size of the particles modified with the polysiloxane shell increased somewhat, while their zeta potential remains almost unchanged. The sedimentation stability of the dispersions of modified particles increased significantly. Attention is also drawn to the weak scattering in the conductivity and zeta potential values measured at several storage times of the dispersions, which also indicates the kinetic stability of the system. A slight decrease in the zeta potential of the CS·D-AspA microparticles during the storage of the dispersions could indicate some deterioration in the quality of the coating or particle aggregation. In general, the particle size and zeta potential of the CS·L-AspA particles were somewhat larger than those of the CS·D-AspA particles.

The functionalization of the surfaces of the nano(micro)particles was verified using the IR method. In the IR spectra of our CS·L-AspA and CS·D-AspA samples isolated from the corresponding associated systems, all characteristic absorption bands typical of this CS salt form, which we described in detail in Ref. [10], were observed. The absorption bands of the Si(OGly)<sub>4</sub> polycondensation product ( $\nu$ ,  $\text{cm}^{-1}$ ) are also clearly visible: for CS·L-AspA, these are 2931 and 2881 (C—H,  $\nu_{\text{as}}$  and  $\nu_{\text{s}}$ ); 1414 ( $\text{CH}_2$ ); and 1151, 1024, and 990 (C—O, Si—O—C, Si—O—Si), while for CS·D-AspA these are 2921 and 2869 (C—H,  $\nu_{\text{as}}$  and  $\nu_{\text{s}}$ ), 1385 ( $\text{CH}_2$ ), and 1148, 1026, and 991 (C—O, Si—O—C, Si—O—Si). The IR spectra of CS·L-AspA and CS·D-AspA indicate the presence of inter- and intramolecular hydrogen contact in the supramolecular structure of our samples. The most informative finding with respect to confirming the formation of bonds between the particles' surfaces and their polysiloxane shells is the wave range from 990 to 1150  $\text{cm}^{-1}$ , within which, in addition to the absorption bands of vibrations of the precursor polycondensation product, the absorption bands of the deformation vibrations of the primary amines associated with the —OH group of the vibration C—O bonds in alcohols and ethers ( $\beta$ -1,4-glucans) and C—O—C bonds, which are predisposed to intermolecular interaction, are also concentrated.

The shapes and average diameters of our chiral nano(micro)particles of CS L- and D-aspartate were also studied via FIB-SEM after the samples were dried on a glass slide. All nanoparticles had a shape that was close to spherical (Figure 2). The largest average characteristic effective diameter (largest transversal size) of CS·L-AspA nanoparticles was  $17.02 \pm 1.25$  nm, while the smallest was  $13.65 \pm 1.28$  nm; for the CS·D-AspA nanoparticles, these values were  $16.25 \pm 3.50$  nm and  $14.84 \pm 1.50$  nm, respectively. The differences in the sizes of the nano(micro)particles determined via DLS and FIB-SEM are typical and are the result of the different conditions present when the dimensional characteristics were estimated. For example, the DLS studies were carried out with dispersions of hydrated particles in water, while the FIB-SEM studies were carried out with air-dried samples.

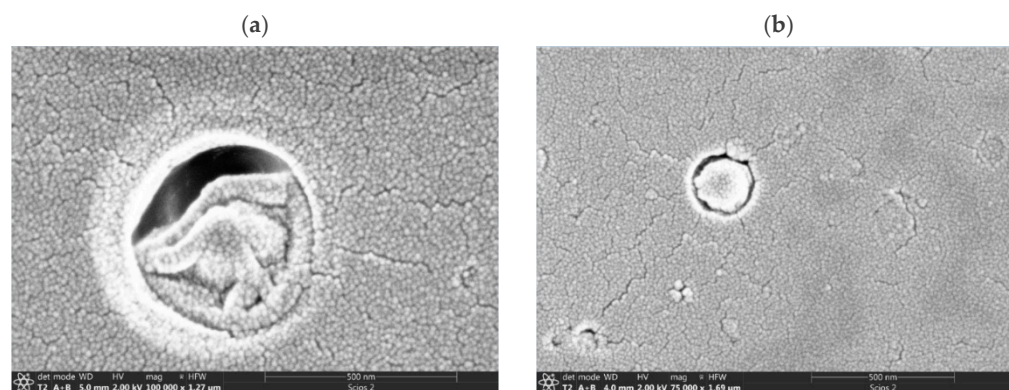


**Figure 2.** FIB-SEM images of chitosan L- (a) and (D-)aspartate (b) nanoparticles modified with a polysiloxane shell.

### 3.2. Biological Properties of Nano(micro)particles of Chitosan L- and D-Aspartate

Special experiments in vitro proved that our chiral nano(micro)particles CS·L-AspA and CS·D-AspA were non-toxic and hemo- and biocompatible.

Experiments conducted in vitro and in vivo revealed that chiral CS·L-(D-)AspA nano(micro)particles are biomimetic with respect to the rhizospheric bacteria *Pseudomonas aureofaciens* and can function as an immunizing elicitor, a curing fungicide, and a protective pesticide. This is expressed in their manifestation of high growth-stimulating activity in relation to the test plants. For example, a comparative assessment of the effect of our nano(micro)particles compared with water on the growth-stimulating activity of radish (*Raphanus sativus*) and mustard (*Sinapis alba*) in the field showed a significant increase in germination, height, and the weight of shoots. Compared to irrigation with water, the increase in green mass and, accordingly, yield through the use of our CS·L-AspA was  $32.0 \pm 2.9\%$  for radish (*Raphanus sativus*) and  $34.4 \pm 3.3\%$  for mustard (*Sinapis alba*), while

those for CS·D-AspA were  $37.9 \pm 5.8\%$  and  $39.3 \pm 1.6\%$ , respectively. Therefore, the greatest effect on biostimulating activity was observed for the CS·D-AspA sample.

#### 4. Conclusions

Thus, our comprehensive study of solutions of CS in L- and D-AspA revealed the effects of counterionic association (self-organization) with the transition of macromolecules to the ionomeric state and the phase segregation of the polymer substance into chiral nano- and microparticles. Optimal conditions for stabilizing particle dispersions through functionalizing their surfaces with a polysiloxane shell have been determined (pharmacologically active silicon tetraglycerolate was used for the first time as a sol–gel precursor). The results obtained demonstrate the promise of using nano(micro)particles of CS L- and D-aspartate not only in biomedical and pharmacological applications but also in agriculture for biological control and increasing crop yields. At the same time, their use does not induce any negative impacts on the environment since the particle formation process involves the use of biologically active raw materials (CS, AspA) without the use of crosslinking reagents and other bio-intolerant chemicals. It is noteworthy that our nano(micro)particles of the homochiral salt complexes D-glucan·D-AspA exhibited the best biostimulating effects.

**Author Contributions:** Conceptualization, methodology, and writing—original draft preparation, A.S.; investigation, data curation, and visualization, X.S., T.L. and T.B. All authors have read and agreed to the published version of the manuscript.

**Funding:** This research was funded by a grant from the Russian Science Foundation № 22-23-00320, <https://rscf.ru/project/22-23-00320/>.

**Institutional Review Board Statement:** Not applicable.

**Informed Consent Statement:** Not applicable.

**Data Availability Statement:** The data presented in this study are available on request from the corresponding author.

**Conflicts of Interest:** The authors declare no conflict of interest.

#### References

1. Chandrasekaran, M.; Kim, K.D.; Chun, S.C. Antibacterial activity of chitosan nanoparticles: A review. *Processes* **2020**, *8*, 1173. [[CrossRef](#)]
2. Cao, S.; Deng, Y.; Zhang, L.; Aleahmad, M. Chitosan nanoparticles, as biological macromolecule-based drug delivery systems to improve the healing potential of artificial neural guidance channels: A review. *Int. J. Biol. Macromol.* **2022**, *201*, 569–579. [[CrossRef](#)] [[PubMed](#)]
3. Hembram, K.C.; Prabha, S.; Chandra, R.; Ahmed, B.; Nimesh, S. Advances in preparation and characterization of chitosan nanoparticles for therapeutics. *Artif. Cells Nanomed. Biotechnol.* **2016**, *44*, 305–314. [[CrossRef](#)] [[PubMed](#)]
4. Hidangmayum, A.; Dwivedi, P. Chitosan based nanoformulation for sustainable agriculture with special reference to abiotic stress: A review. *J. Polym. Environ.* **2022**, *30*, 1264–1283. [[CrossRef](#)]
5. Negi, A.; Kesari, K.K. Chitosan nanoparticle encapsulation of antibacterial essential oils. *Micromachines* **2022**, *13*, 1265. [[CrossRef](#)] [[PubMed](#)]
6. Rossi, S.; Vigani, B.; Puccio, A.; Bonferoni, M.C.; Sandri, G.; Ferrari, F. Chitosan ascorbate nanoparticles for the vaginal delivery of antibiotic drugs in atrophic vaginitis. *Mar. Drugs* **2017**, *15*, 319. [[CrossRef](#)] [[PubMed](#)]
7. Puccio, A.; Ferrari, F.; Rossi, S.; Bonferoni, M.C.; Sandri, G.; Dacarro, C.; Grisoli, P.; Caramella, C. Comparison of functional and biological properties of chitosan and hyaluronic acid, to be used for the treatment of mucositis in cancer patients. *J. Drug Deliv. Sci. Technol.* **2011**, *21*, 241–247. [[CrossRef](#)]
8. Luangtana-anan, M.; Nunthanid, J.; Limmatvapirat, S. Potential of different salt forming agents on the formation of chitosan nanoparticles as carriers for protein drug delivery systems. *J. Pharm. Investig.* **2019**, *49*, 37–44. [[CrossRef](#)]
9. Shipovskaya, A.B.; Lugovitskaya, T.N.; Zudina, I.V. Biocidal activity of chitosan aspartate nanoparticles. *Microbiology* **2023**, *92*, 75–82. [[CrossRef](#)]
10. Lugovitskaya, T.N.; Shipovskaya, A.B.; Shmakov, S.L.; Shipenok, X.M. Formation, structure, properties of chitosan aspartate and metastable state of its solutions for obtaining nanoparticles. *Carbohydr. Polym.* **2022**, *277*, 118773. [[CrossRef](#)] [[PubMed](#)]
11. Shipovskaya, A.B.; Gegel, N.O.; Shipenok, X.M.; Ushakova, O.S.; Lugovitskaya, T.N.; Zudina, I.V. Structure, properties and biological activity of chitosan salts with L- and D-aspartic acid. *Biol. Life Sci. Forum* **2022**, *20*, 5. [[CrossRef](#)]

12. Gegel, N.O.; Zhuravleva, Y.Y.; Shipovskaya, A.B.; Malinkina, O.N.; Zudina, I.V. Influence of chitosan ascorbate chirality on the gelation kinetics and properties of silicon-chitosan-containing glycerohydrogels. *Polymers* **2018**, *10*, 259. [[CrossRef](#)] [[PubMed](#)]
13. Shadrina, E.V.; Malinkina, O.N.; Khonina, T.G.; Shipovskaya, A.B.; Fomina, V.I.; Larchenko, E.Y.; Popova, N.A.; Zyryanova, I.G.; Larionov, L.P. Formation and pharmacological activity of silicon—Chitosan-containing glycerohydrogels obtained by biomimetic mineralization. *Russ. Chem. Bull.* **2015**, *64*, 1633–1639. [[CrossRef](#)]
14. Jesus, S.; Marques, A.P.; Duarte, A.; Soares, E.; Costa, J.P.; Colaço, M.; Schmutz, M.; Som, C.; Borchard, G.; Wick, P.; et al. Chitosan nanoparticles: Shedding light on immunotoxicity and hemocompatibility. *Front. Bioeng. Biotechnol.* **2020**, *8*, 100. [[CrossRef](#)] [[PubMed](#)]

**Disclaimer/Publisher’s Note:** The statements, opinions and data contained in all publications are solely those of the individual author(s) and contributor(s) and not of MDPI and/or the editor(s). MDPI and/or the editor(s) disclaim responsibility for any injury to people or property resulting from any ideas, methods, instructions or products referred to in the content.